NASA/JPL AI RSAR: SYSTEM OVERVIEW AND INTRODUCTION '1'0 DATA INTERPRETATION

MAHTA MOGH ADDAM

JET PROPULSION LABORATORY
CALIFORNIA INSTITUTE OF TECHNOLOGY
4800 OAK GROVE DRIVE
PASADENA, CA 91109

ABSTRACT

The JPL airborne synthetic aperture radar (AIR SAR) is a quadpol system operating at threw frequencies, which measures the complete stokes matrix of scattering targets and hence their polarization signature. The high resolution of AIRSAR, in additi on to its ability to penetrate cloud and smoke cover, make it the remote sensing instrument of choice for use over a variety of scenes, ranging from bare soil surfaces to tropical forests. In this work, a description of the AI RSAR system characteristics and parameters will be given, followed by an introduction to the most recent advancements in the interpretation of SAR data for ecological and physiological application and quantitative estimation of scattering scene parameters.

INTRODUCTION

The use of synthetic aperture radar (SAR) in remote sensing has gained significant attention recently due to its flexibility of data acquisition and the wealth of information provided. SAR utilizes active microwave illumination which penetrates cloud and smoke cover, in contrast to other instruments such as optical and infrared devices, thus making it possible to study and monitor scenes ranging from arid soil surfaces to dense tropical rainforests around the glob independent of seasonal changes, weather conditions, and geographical loc ations. Furthermore, if the measurements are done in a polarimetric fashion, it may be possible to obtain more detailed information about scattering and struc tural properties of the ground targets via theoretical models (Durden et al, 1988, Cihlar et al., 1992, Dobson et al., 1992, Hess et al., 1990, Sun et al., 1988).

Recent technological advances have per mitted the use of polarimetry in radar imaging systems. One such system is the NASA/JPL airborne synthetic aperture radar (AIR SAR), which uses a DC-8 aircraft platform. The AIRSAR operates at C-, 1)-, and P-bands (5.6 cm, 9 4 cm, and 68 cm wavelengths, respectively) with a 20 MHz or 40 MHZ bandwidth. It measures four transmit-receive polarization combinations, which yield the full Stokes matrix of scattering cells and hence the full polarization signature of the remote targets. For any transmit polarization of the electromagnetic field, the received signal, or the scattered field, is in general a vector quantity and possesses a general polarization that can be described as a combination of two orthogonal polarizations (for a plane wave). Hence, by making measurements of two independent receive polarizations for each transmitted signal, it is possible to define the scattered field completely for any point in space where the measurements are taken. Electromagnetic scattering models relate the electrical parameters of objects to the full vector transmitted and received fields, hence such polarimetric knowledge is necessary to infer various scattering properties of the remote targets which cannot be obtained through single polarization channel measurements.

The JPL AIR SAR, though being continuously improved and optimized, is now in an operational state. The hardware, calibration procedures, data storage techniques, and processing; algorithms arc fully developed and standardized to a large degree. The current challenge, however, is in the area of interpreting the data and applying the results in related scientific fields such as ecology and geophysics. Among such applications arc classification of vegetation growth and land use, generation of surface elevation maps, and quantitative electromagnetic inversion to obtain specific scattering information about various scenes.

In this work, a brief review of concepts of SAR will be given, followed by some specifics of the JPL AIRSAR system. Some current and potential applications of the SAR data will then be discussed. Due to space limitation, only a small list of references can be provided. For more information, the reader is encouraged to refer to Zebker and van Zyl (1991) and Moghaddam (1993a).

SAR SYSTEM DESIGN

Polarimetric Data Acquisition

The present AIRSAR design is based on the JPL CV-990, which served as the prototype polarimetric radar operating at L-band only (Zebker and van Zyl, 1991, Ulaby and Elachi, 1990). The radar alternatively transmits vertical (V) and horizontal (H) linearly polarized waves, and simultaneously receives both polarizations, hence measuring the four elements of the scattering matrix. A block diagram of this system is given in Figure 1. The adjacent V and H transmit pulses are separated by 0.51 ms in time. Several pulses corresponding to the different polarization combinations are coherently integrated to form a synthetic aperture. The interspersed pulses form four spatial arrays which are partially decorelated since they arc not measured simultaneously. Hence, each corresponding patch of the probed surface is viewed at a slightly different angle. This gives rise to the "speckle" effect. This is a minor problem for the AIR SAR, as the distance traveled by the aircraft in the interpulse period is small compared to the resolution cell size.

Calibration

Relative and absolute calibration of the various channels in a polarimeter is a crucial issue, especially if the measurements are to be used in quantitative theoretical analyses. To insure accurate results, the following have to be performed: 1) antenna pattern correction, 2) phase calibration, 3) channel imbalance removal, 4) cross talk removal, and 5) absolute amplitude calibration. Currently, calibration targets, namely, trihedral corner reflectors are deployed at flight sites to perform the above steps. If the topography of the imaged area is known, it is also possible to remove the effect of pixel heights in the normalized radar return.

Data Processing

Figure 2 shows the SAR processor data flow (Ulaby and Elachi, 1990): Data are read from high-density digital tapes that were written during the flight. The echoes in the range (cross track) direction are compressed by a convolution with a range reference function. To reduce the storage volume, data are presummed by a factor of four and Fourier transformed in the azimuth (along track) direction. Then a range interpolation is performed along the curves of the range history for targets at each desired output range. An azimuth reference function is multiplied by the results and inverse transformed to produce the final output for each of the channels (Ulaby et al., 1986a). The polarimetric data are stored in Stokes matrix format, described below.

DATA STORAGE FORMAT

Stokes Matrix Representation

For data storage efficiency, the measured scattering matrix elements for each resolution cell, or pixel, are transformed into Stokes matrix elements and compressed in such a way as to occupy only 10 storage bytes. The Stokes matrix elements are linear combinations of crossproducts of the four scattering matrix elements, hence the full polarimetric scattering information is preserved (Zebker and van Zyl, 1 991). The matrix has 9 independent elements, each a real number. A quantization technique is used such that the nine real numbers (36 bytes) can be equivalently stored in 10 bytes, significantly reducing the large data volume (a typical SAR image contains 1280 range lines, each 1024 pixels wide).

Polarizaton Signatures

From the Stokes matrix polarimetric representation of the measured backscattered fields, it is possible to construct the "polarization signature" which is a graphical representation of the behavior of the received power as a function of polarization parameters, namely, ellipticity and orientation angles of the transmitted signal. An example is given in Figure 3 for the signature of a perfectly conducting dihedral corner reflector, where, e.g., it can be seen that the backscatter return is at a minimum for ellipticity angles of 0° and orientation anlges of 45° and 135°.

APPLICATIONS AND DATA INTERPRETATION

With the development of advanced polarimetric radar systems in the recent years, many new applications have evolved which have improved or possess the potential to improve our understanding of the global environment and its trends of change.

Microwave frequencies are capable of penetrating cloud cover which debilitates remote sensing instruments operating at optical frequencies. Signals at lower frequencies, such as P-band, may even penetrate vegetation covers and the returned signals may contain information about the lower layers of vegetation and the ground underneath. Furthermore, the availability of full polarimetric measurements provides for possible inference of target electrical and structural properties. These features make the SAR the remote sensing instrument of choice over such varied scenes as bare or arid soil surfaces, rocks, agricultural areas, forested areas, sea surface, and glaciers.

Classification

Researchers have used many techniques for distinguishing between various land-use types by utilizing statistical as well as simplified scattering models which relate the radar backscatter to the properties of ground targets. For example, Ulaby et al. (1 9861.,) have used statistical characteristics present in radar images to relate variability of radar backscatter values to such scene properties as "texture" (intrinsic spatial variability) as opposed to "fading" (speckle). They have deduced that texture information can be used to achieve high accuracy classification between many vegetation types. An example of using simplified scattering theories for classification is the 3-component model developed by Freeman and Durden (1 992) and a similar one by van Zyl (1989), which identifies the three major scattering processes (surface, volume, and double-bounce), and depending on the contribution of each mechanism, classifies the vegetation and land-use type in any location within an image.

Interferometry

Another highly active and important application of radar is mapping surface elevation by using techniques such as interferometry, where two images are constructed of a scene by flying two spatially separated antennas (Evans et al, 1993). The phase difference between the two received signals is computed and related to height of each image pixel. If the wavelength is small enough, as in C-band, the two antennas can be mounted on the airplane and flown simultaneously, as is done in TOPSAR. For larger wavelengths (L- and P- bands), it is possible to make repeat passes over the area to be imaged, where tile flight tracks arc separated by the proper amount, and are known with proper accuracy.

Modelling and Inversion

One of the main current challenges in quantitative interpretation of SAR data is the development of methods for inferring scattering parameters of ground targets from polarimetric backscattering measurements. The knowledge of these quantities is the key to understanding and monitoring the Earth's environment and resources on a local and global scale. These are properties such as soil moisture (equivalently, dielectric constant), vegetation water content, surface roughness, tree density and heights in forests, dielectric. constant of tree components, and canopy density. The radar backscatter data are related to these parameters through electromagnetic scattering models (see, for instance, Tsang et al., 1985). Several Such models have been developed and their results using ground-truth measurements have been compared to radar data. For instance, for forested areas there mist several models among which arc the discrete scatterer model which takes the forest as consisting of horizontal layers of cylinders to simulate branches and trunks, and a rough surface to model the forest floor (Durden et al., 1989 and 1991). Radiative transfer theory has also been used in other models such as MIMICS from the University of Michigan (Ulaby et al., 1990 b). A comparison of the polarization signature of a forested area calculated from the former model for an area near Moosehead Lake, Maine, and the actual radar measurement is shown in Figure 4, where it is seen that the two signatures are in good agreement.

In principle, it is possible to calculate the scattering parameters used in the models from scattering data. We call this process "inversion." In practice, however, the theoretical models prove to be too complex and involve too many parameters to be feasibly inverted. The number of available data points for each pixel in an image is nine (3 frequencies and 3 independent polarizations), whereas the number of unknowns is typically many times more. Recently, an approach has been proposed for reducing the number of unknown parameters to make inversion possible (Moghaddam et al., 1993b). The method is based on performing a classification initially to identify dominant scattering mechanisms in each area. The scattering model is then reduced to that containing the component of the dominant mechanism, thereby limiting the number of unknowns. For example, if the scattering from an area is identified as that due to a surface, only unknowns describing the surface (dielectric constant and roughness measures) need to be found.

Once the scattering mechanisms are identified, the appropriate parameterized model can be used along with an inversion algorithm to obtain the unknowns. Assuming a parameterized model for the given situation is at hand (nontrivial), an inversion based on nonlinear optimization must be performed. The process is nonlinear, since the unknowns and measurements are in general related in a nonlinear fashion. The inverse problem can be stated as the problem of finding the unknowns such that the model predictions and radar measurements are "close." Denoting the unknowns as elements of the vector **X**, the nonlinear model as f_{nl} and the measured data as d_{meas}, the inverse problem is equivalently stated as finding **X** such that a least-squares measure

$L(\mathbf{X})$ given by

$$L(x) = \frac{1}{2}\{\|\mathbf{f}_{nl}(\mathbf{X}) - \mathbf{d}_{meas}\|^2 + \|\mathbf{X} - \mathbf{X}_{ap}\|^2\}$$

is minimized. Here, $\mathbf{X}_{ap}$ is an a priori estimate of X, which could be arbitrarily different from the true solution for X. Once the proper stochastic properties of the unknowns and measurements are taken into account, the above optimization problem can be solved via iterative techniques (Moghaddam, 1993b).

AIRSAR AS PROTOTYPE FOR SPACEBORNE SYSTEMS

The airborne L- and C-band SAR have served as the prototypes for the spaceborne SAR, SIR-C/X-SAR, scheduled to fly in April and August of 1994 (Evans et al., 1993). The mission is a collaboration between NASA, the German Space Agency, and the Italian Space Agency, and is a continuation of NASA's spaceborne imaging radar (SIR) program with Seasat (1978), SIR-A (1981), and SIR-B (1984) as its predecessors. SIR-C/X-SAR will have full polarimetric capabilities and equipped with L-, C-, and X-bands. It will provide global coverage on a rapid temporal scale, and will image at multiple aspect and incidence angles. The campaign will provide valuable data for use in algorithms (such as that described above) to obtain key geophysical products to study global change. The research topics will include the global carbon cycle, paleoclimate and geologic processes, ocean circulation, air-sea interactions, and advanced technology. To address these issues, essential in answering critical environmental problems, several supersites have been chosen around the world.

The SAR topographic interferometer (TOPSAR) has also provided a prototype for the spaceborne system TOPSAT. NASA has been studying options for realization of a spaceborne system to produce accurate global topographical maps through missions such as Seasat, SIR-A, SIR-B, and AIRSAR, and will use SIR-C in a repeat pass scheme. Several implementation possibilities are currently under consideration. The purpose of such mission is to obtain a complete and uniform high resolution map of nearly 90% of the Earth's land mass with high spatial resolution and high vertical accuracy. As such, the system will increase topographic knowledge by 1 to 2 orders of magnitude over existing data base. Global coverage will be provided over a period of six months. In addition to the Earth's topography, it may be possible to obtain vegetation height maps and surface roughness maps for global change studies.

SUMMARY

SAR is an indispensable tool for mapping and monitoring the Earth's resources and environment on a local and global scale. It provides a means of acquiring remotely sensed data complementary to those obtained by visible, near infrared, and thermal infrared portions of the Electromagnetic spectrum. Technological advances have made polarimetric SAR an operational and reliable instrument, and advanced processing and calibration algorithms are now standardized to readily provide scattering data useful in scientific computations. The current challenges in this area are devising new applications and new algorithms for interpretation of SAR data, among which inversion for geophysical parameters is perhaps the most essential for global change studies. The technology and analysis tools for the airborne system have served as the evolutionary predecessors of the spaceborne instruments such as SIR-C/X-SAR and TOPSAT.

Acknowledgement

The work described here was performed by the Jet Propulsion Laboratory, California Institute of Technology, under a contract from the National Aeronautics and Space Administration.

REFERENCES

Cihlar, J., 'T'. J. Pultz, and A. L. Gray, (1992), Change detection with synthetic aperture radar. *Int. J. Remote Sensing*, 13: 401-414.

Dobson et al., (1992), Dependence of radar backscatter on conifer forest biomass, *IEEE Trans. Geosci. Remote Sensing*, **30: 4** 12-415.

Durden, S. L., H. A. Zebker, and J. J. van Zyl, (1988), Application of radar polarimetry to forestry. *Proc. IGARSS '68 Symposium*, Edinburgh, Scotland, **1003-1004.**

Durden, S. L., J. J. van Zyl, and H. A. Zebker, (1989), Modeling and observation of the radar polarization signature of forested areas. *IEEE Trans. Geosci. Remote Sensing*, 27: 290-301.

Durden, S. L., J. D. Klein, and H. A. Zebker, (1991), Polarimetric radar measurements of a forested area near Mt. Shasta. *IEEE Trans. Geosci. Remote sensing*, 29: 444-450.

Evans, D. L. et al., (1992), Radar interferometry studies of the Earth's topography. *EOS Trans.*, 73: **557-558.**

Evans, D. L. et al., (1993), The shuttle imaging radar-C and X-SAR mission. *EOS Trans.*, **74: 145, 157-158.**

Freeman, A., S. L. Durden, and R. Zimmermann, (1992), Mapping subtropical vegetation using multifrequency, multipolarization SAR data. *Proc. IGARSS'92*, Houston, TX, 1 **GM-1689.**

Hess, L. L., J. M. Melack, and D. S. Simonett, (1990), Radar detection of flooding beneath the forest canopy: A review. *Int. J. Remote Sensing*, 11: 1313-1325.

Moghaddam, M., S. L. Durden, and H. A. Zebker, (1993a), Radar measurement of forested areas during OTTER. *Remote Sens. Environ.*, in press.

Moghaddam, M. and S. Saatchi, (1993b), An inversion algorithm applied to SAR data to retrieve surface parameters. *Proc. IGARSS '93*, Tokyo, Japan, **587-589.**

Sun, **G. Q.,** and D. **S.** Simonett, (1988), Simulation of L-band HH microwave backscattering from coniferous forest stands: a comparison with S11{-1] data. *Int. J. Remote Sensing*, 9: 907-925.

Tsang, L., J. A. Kong, and R. T. Shin, (1985). *Theory of Microwave Remote Sensing.*

New York: Wiley-Illtcrsciellcc.

Ulaby, F. T., R. K. Moore, and A. I{. Fung, (1986a). Microwave *Remote Sensing: Active and Passive.* Dedham, MA: Artech House, Inc.

Ulaby, F. T., F. Kouyate, B. Brisco, and '1'. H. Lee Williams, (1986b), Textural information in SAR images. *IEEE Trans. Geosci. Remote Sensing*, 24: 235-245.

Ulaby, F. '.'. and C. Elachi, (1990a), Radar Polarimetry for Geoscience Applications. Norwood, M A: Artech H ouse, Inc.

Ulaby, F. T., K. Sarabandi, K. McDonald, M. Witt, and M . C. Dobson, (1990b), Michigan microwave canopy scattering model (MIMICS). *Int. J. Remote Sensing.*

van Zyl, J. J., H. A. Zebker, and C. Elachi, (1 987), Imaging radar polarization signatures: Theory and observation. *Radio Sci.*, 22: 529-543.

van Zyl, J. J., (1 989), Unsupervised classification] of scattering behavior using radar polari net ry data. *IEEE Trans. Geosci. Remote Sensing*, 27: 36-45.

Zebker, H., and J. J. van Zyl, (1991), Imaging radar polarimetry: A review. *IEEE Proc.*, 79: 1583-1606.

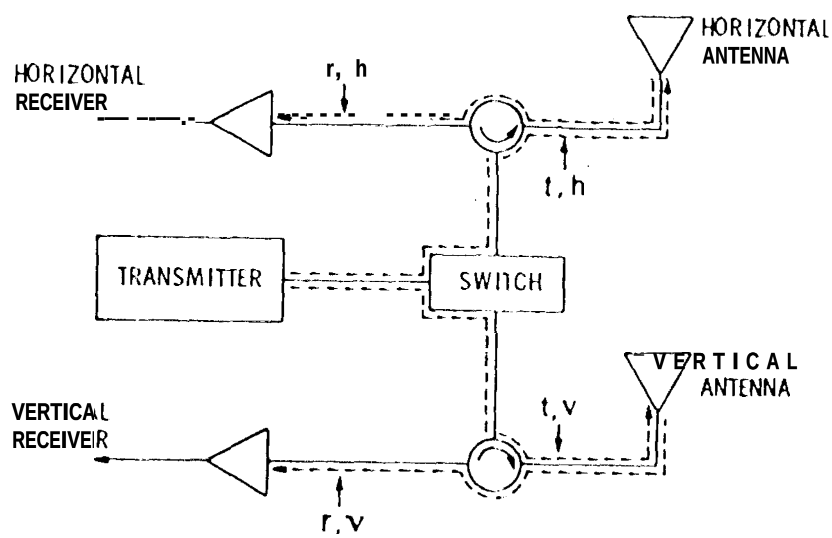

Figure 1. Block diagram of a polarimeter

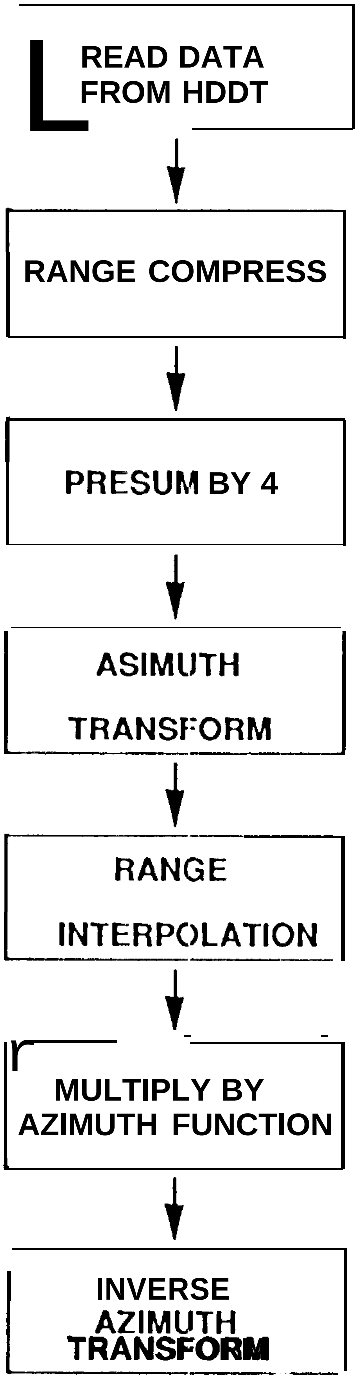

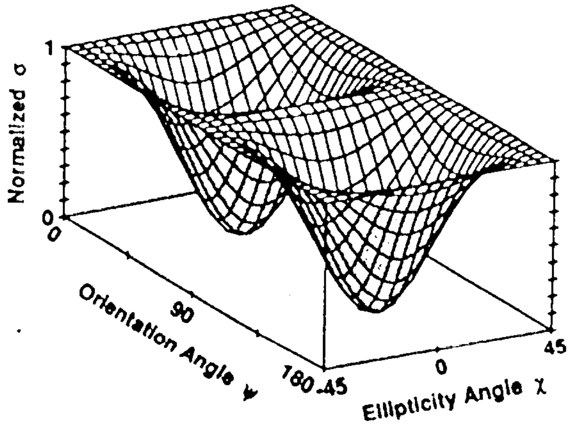

Figure 3. Polarization signature of a perfectly conducting dihedral corner reflec tor.

Figure 2. SAR processor data flow diagram.

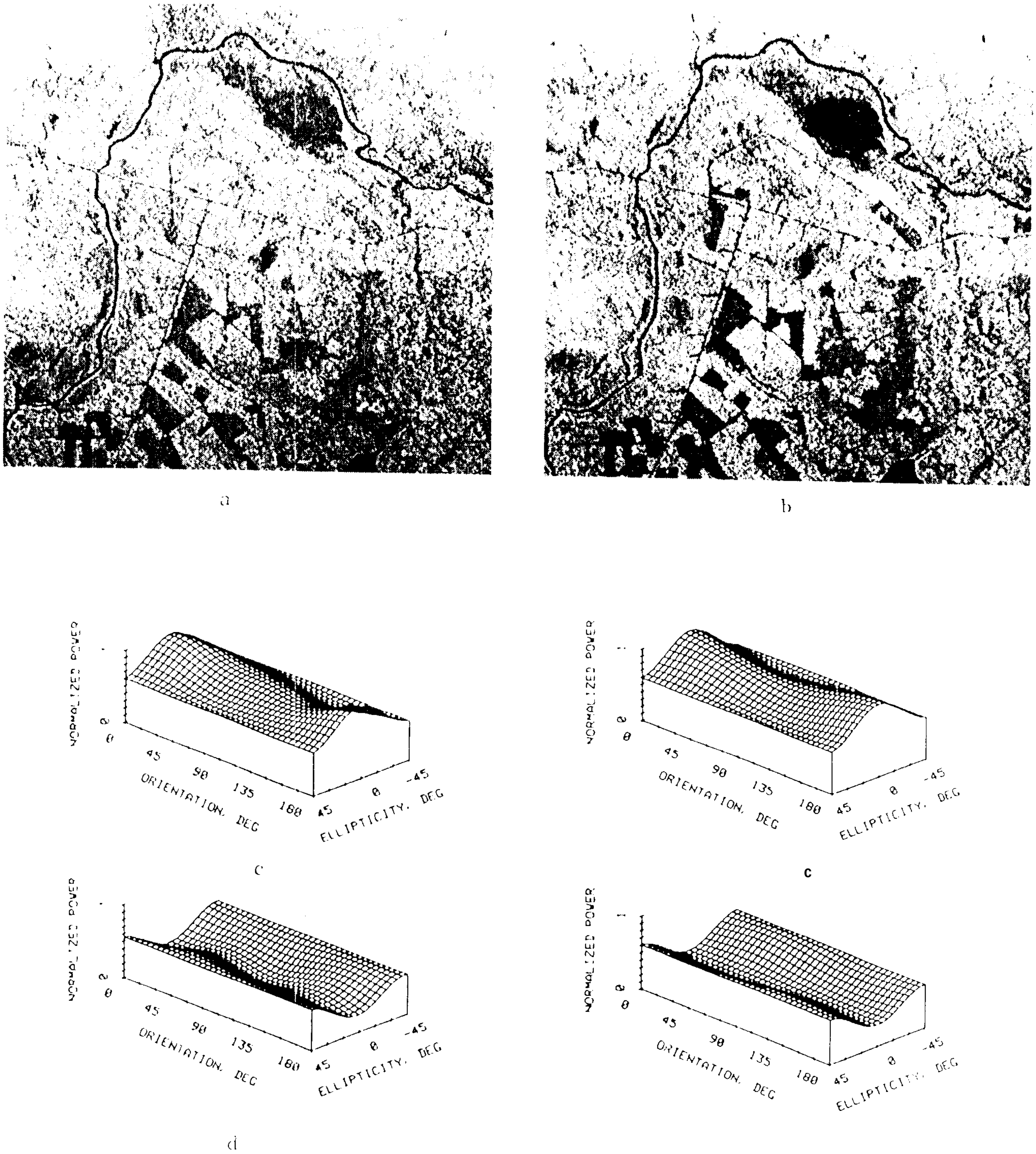

Figure 4. (a) L-band HH SAR image obtained over the area near Moosehead Lake, ME. (b) L-band HV SAR image over the same area. (c) Observed copolarized signature over a forested area in (a-b). (d) Observed crosspolarized signature over forested area. (e) Calculated copolarized signature for (c). (f) Calculated crosspolarized signature for (d).